25th ABCM International Congress of Mechanical Engineering
October 20-25, 2019, Uberlândia, MG, Brazil

COBEM2019-0542
A SURROGATE MODEL BASED ON PROPER ORTHOGONAL DECOMPOSITION AND RADIAL BASIS FUNCTIONS FOR THE ANALYSIS OF PHASE CHANGE MATERIALS CONTAINING NANOPARTICLES

Bruno dos Reis Jaccoud
Department of Nanotechnology Engineering - COPPE/UFRJ, Caixa Postal 68501, Cidade Universitária, Rio de Janeiro-RJ, 21941-972, Brazil
bruno.jaccoud@gmail.com
Helcio R. B. Orlande
Marcelo J. Colaço
Department of Mechanical Engineering – COPPE/UFRJ, CP 68503, CT, Federal University of Rio de Janeiro, Rio de Janeiro-RJ, 21941-972, Brazil
helcio@mecanica.ufrj.br
colaco@mecanica.coppe.ufrj.br
Ryszard Bialecki
Zbigniew Buliński
Ziemowit Ostrowski
Institute of Thermal Technology, Silesian University of Technology ul. Konarskiego 22, 44-100 Gliwice
ryszard.Bialecki@polsl.pl
zbigniew.Bulinski@polsl.pl
ziemowit.Ostrowski@polsl.pl

Abstract. *Considerable amount of thermal energy can be stored when a material undergoes phase change, with melting temperatures that can be suitable for several practical applications, like in solar energy. Recently, nanoparticles dissolved in the PCM have been used to enhance the thermal storage. This work deals with the numerical simulation of PCM's containing nanoparticles, used for the thermal storage of solar energy. Energy, momentum and mass conservation equations were solved numerically with finite volumes and the enthalpy method, for a two-dimensional rectangular geometry, taking into account buoyancy effects. The PCM adopted was a paraffin ($C_{28}H_{58}$) containing copper nanoparticles (1% volume concentration). The main objective of this work was to introduce a surrogate model for this problem, aiming at a drastic reduction of computational time, which can allow for future online state estimation with Bayesian techniques, like the Particle Filter. The surrogate model was based on the Proper Orthogonal Decomposition and Radial Basis Functions. The complete model solution, obtained with a finite volume computer code, was used to generate the POD basis. The coefficients for the POD basis were then expressed as a linear combination of radial basis functions, for the variables of interest.*

Keywords: *phase change material, solar energy storage, surrogate model, proper orthogonal decomposition, radial basis functions*

1. INTRODUCTION

Energy from different renewable sources is currently used in large scale worldwide. However, due to the uncertain supply of renewable energy sources, storage of energy is of major importance for their practical use (Fernandes et al, 2012). Considerable amount of thermal energy can be stored when a material undergoes phase change. Paraffin, water, salt hydrates and sugar alcohols are examples of phase change materials (PCMs) with high latent heat and with melting temperatures that can be suitable for several practical applications (Yousef et al, 2013). Therefore, PCMs can be used for thermal energy storage, particularly for solar applications where the energy supply is intermittent during the day and the demand peak can be at times where the sun light is not available. The PCM can be appropriately selected for a specific application based on its phase change temperature (Yousef et al, 2013 and Dhaidan et al, 2013). More recently, nanoparticles made of different materials, such as CuO, Cu, Al_2O_3, TiO_2, Al, Graphene, Graphite, carbon nanotubes, SiO_2 or ZnO, dissolved in the base PCM, have been used for enhancing the thermal energy storage.

This work deals with the numerical simulation of phase change in materials containing nanoparticles, applied for the thermal storage of solar energy. A rectangular cavity filled with the phase change material is heated through one its boundaries with a solar heat flux typical of the city of Rio de Janeiro (Miller and Colaço, 2016). The numerical simulation is performed with the model advanced by Colaço and Dulikravich (2007, 2008), which is based on the finite volume method and the enthalpy formulation of the energy equation. The solute transport in the solid and liquid phases is accounted for, as well as natural convection in the liquid region. Due to the iterative character of the enthalpy method, together with the pressure-velocity coupling scheme used to solve the mass and momentum conservation equations, the numerical solutions for the cases of interest in this work are very time consuming.

The amount of energy stored in PCMs is of great interest for practical applications. Although such quantity can be dynamically estimated with the time integration of measured heat fluxes, the solution of inverse problems based on non-intrusive temperature measurements can be a robust and accurate prediction technique. Inverse problems rely on measurements of dependent variables of the mathematical formulation of the physical problem, for the estimation of parameters or functions appearing in this formulation (Özışık and Orlande, 2000; Colaço et al, 2006; Orlande et al, 2011). The numerical solution of the mathematical formulation of the physical problem must be computed several times for the solution of inverse problems. Therefore, the use of inverse analyses for the estimation of the amount of energy stored in phase change materials might not be possible for practical applications, due to the large computational time required for the solution of the phase change direct problem.

This paper is not aimed at the solution of inverse problems, but at obtaining fast solutions of the direct problem, which would allow real time estimation of the amount of energy thermally stored in phase change materials. The main objective of this work is to obtain a surrogate solution of the phase change problem, based on Proper Orthogonal Decomposition (POD) and Radial Basis Functions (RBF), such as in (Ostrowski, 2006). Since then, the technique was advanced and successfully used as a surrogate model (Ostrowski, 2006; Rogers et al, 2008, 2012). In fact, POD can be used to produce a low-order, but highly accurate, approximation of the solution (Rogers et al, 2012). This technique is capable of capturing dominant components (called principal components) of the data, since POD selects the best basis for a least-squares approximation that defines a set of vectors (Rogers, 2008). The surrogate solution, obtained for specific sets of input parameters used for the complete solution, can be accurately extended to other parameter values by using an interpolation with Radial Basis Functions (RBF), as demonstrated in (Ostrowski, 2006).

2. PHYSICAL PROBLEM AND MATHEMATICAL FORMULATION

The physical problem examined in this paper involves the phase change of a base material containing nanoparticles inside a square cavity, as illustrated by Fig. 1. The material is initially in the solid phase, with a uniform concentration of nanoparticles and at a uniform temperature below the melting temperature. At time zero, the left surface is subjected to time-dependent heat flux $q(x,t)$, while the other boundaries are supposed as thermally insulated solid walls (see Fig. 1). The heat flux imposed at the left boundary is presented by Fig. 2. The heat flux during the heating period corresponds to the typical solar irradiation at the city of Rio de Janeiro in February (Miller, and Colaço, 2016). The heat flux during the cooling period is assumed in this work as constant and represents an average night consumption of the stored energy. The phase change material properties are assumed constant, except for the density in the buoyancy term, where we consider Boussinesq's approximation valid for laminar natural convection.

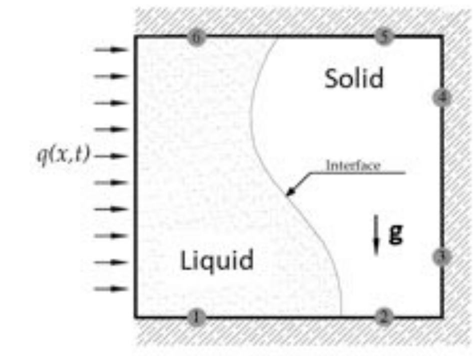

Figure 1. Sketch of the physical problem.

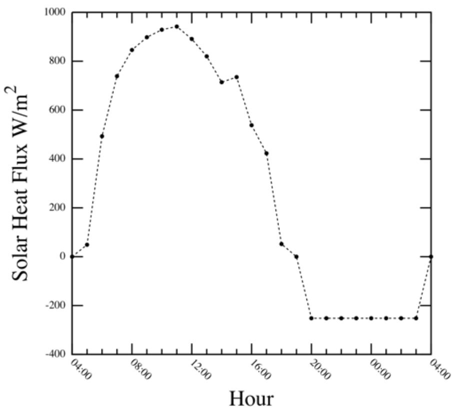

Figure 2. Solar Heat Flux (Modified from (Miller and Colaço, 2016)).

The general conservation equation for a variable φ can be written as (Colaço and Dulikravich, 2007; Voller et al, 1989; Zabaras and Samanta, 2004):

$$\frac{\partial}{\partial t}(g_s\rho_s\varphi_s + g_l\rho_l\varphi_l) + \nabla\cdot(g_s\rho_s\mathbf{u}_s\varphi_s + g_l\rho_l\mathbf{u}_l\varphi_l) = \nabla\cdot(g_s\Gamma_s^\varphi\nabla\varphi_s + g_l\Gamma_l^\varphi\nabla\varphi_l) + F_s + F_l \tag{1}$$

where g is the volume fraction, ρ is the density, Γ is the diffusion coefficient, $\mathbf{u}$ is the velocity vector, F is the body force, and the subscripts s and l refer to the liquid and solid phases, respectively. The volume fractions g_s and g_l are related to the mass fractions, f_s and f_l, by (Colaço and Dulikravich, 2007; Voller et al, 1989; Zabaras and Samanta, 2004):

$$\rho f_s = \rho_s g_s \tag{2}$$

$$\rho f_s = \rho_s g_s \quad , \quad \rho f_l = \rho_l g_l \tag{3}$$

where the local mixture density is defined as

$$\rho = \rho_s g_s + \rho_l g_l \tag{4}$$

It is assumed here that $\rho_s = \rho_l$ (Colaço and Dulikravich, 2007; Voller et al, 1989; Zabaras and Samanta, 2004). Moreover, the solid and the liquid are assumed to have the same local velocity, that is,

$$\mathbf{u} = \mathbf{u}_s = \mathbf{u}_l \tag{5}$$

and Eq.(1) can be written as:

$$\frac{\partial}{\partial t}(\rho\varphi) + \nabla\cdot(\rho\varphi\mathbf{u}) = \nabla\cdot(\Gamma^\varphi\nabla\varphi) + F \tag{6}$$

where

$$\Gamma^\varphi = g_s\Gamma_s^\varphi + g_l\Gamma_l^\varphi \tag{7}$$

$$F = F_s + F_l \tag{8}$$

The concentration of nanoparticles within the solid and liquid phases, $\varphi_s = C_s$ and $\varphi_l = C_l$, respectively, follow a binary diagram. In the mushy region, the concentrations of nanoparticles in the liquid and solid phases are related through the partition coefficient, κ, defined as (Colaço and Dulikravich, 2007):

$$C_s = \kappa C_l \tag{9}$$

where $0 < \kappa < 1$ and the *liquidus* and *solidus* curves are assumed as straight lines (see Fig. 3), given respectively by:

$$C_{liq} = \frac{T_m - T}{T_m - T_{eut}} C_{eut} \tag{10}$$

$$C_{sol} = \frac{T_m - T}{T_m - T_{eut}} \kappa C_{eut} \tag{11}$$

Therefore, for $C < C_{eut}$, the *liquidus* and *solidus* temperatures are given respectively by:

$$T_{liq} = T_m - (T_m - T_{eut})\frac{C}{C_{eut}} \tag{12}$$

$$T_{sol} = \max\left[T_{eut}, T_m - (T_m - T_{eut})\frac{C}{\kappa C_{eut}} \right] \tag{13}$$

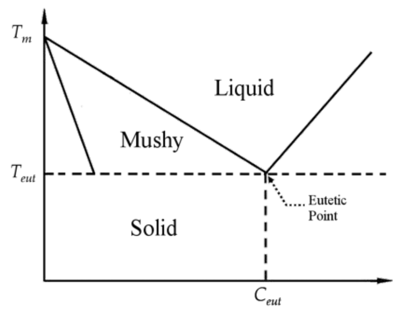

Figure 3. A binary diagram with straight *solidus* and *liquidus* lines.

The solid fraction in the mushy region was modeled in this work by the Lever Rule (Rappaz, 1989) , that is,

$$f_s = \frac{1}{1-\kappa}\left(\frac{T_{liq} - T}{T_m - T} \right) \tag{14}$$

which assumes complete mixing in both liquid and solid phases. Note that, as the solidification begins, the solid phase rejects solute and its concentration in the remaining liquid phase, and especially in the mushy region, increases.

In this work we use the enthalpy formulation of the energy equation, which is given by (Colaço and Dulikravich, 2007; Orlande et al, 2017):

$$\frac{\partial}{\partial t}(g_s \rho_s h_s + g_l \rho_l h_l) + \nabla \cdot (g_s \rho_s \mathbf{u}_s h_s + g_l \rho_l \mathbf{u}_l h_l) = \nabla \cdot (g_s k_s \nabla T_s + g_l k_l \nabla T_l) \tag{15}$$

By assuming constant density and defining

$$h = g_s h_s + g_l h_l \tag{16}$$

$$k = g_s k_s + g_l k_l \tag{17}$$

Eq. (15) can be written as

$$\frac{\partial}{\partial t}(\rho h)+\nabla\cdot(\rho\mathbf{u}h)=(k\nabla T) \tag{18}$$

3. SURROGATE MODEL BASED ON PROPER ORTHOGONAL DECOMPOSITION AND RADIAL BASIS FUNCTIONS (POD-RBF)

The POD-RBF surrogate model requires the so-called snapshots. A snapshot $\mathbf{s}$ contains N values of the field under analysis. A collection of M snapshots $\mathbf{s}^j, j=1,2,\ldots,M$, is generated by sampling the prior statistical distributions of the input parameters upon which the field depends on. Each $\mathbf{s}^j$ is then saved as a column of the rectangular matrix $\mathbf{S}$, denoted as the snapshot matrix, of size $N\times M$.

The aim of POD is to construct a small set of orthonormal vectors $\bar{\mathbf{\Phi}}$ representing the original matrix $\mathbf{S}$ in an optimal way (Ostrowski et al, 2005; Ostrowski et al, 2008), that is,

$$\mathbf{S}=\bar{\mathbf{\Phi}}\bar{\mathbf{A}} \tag{19}$$

where $\bar{\mathbf{A}}$ is the matrix of amplitudes of the expansion and $\bar{\mathbf{\Phi}}$ is the truncated POD basis, which is orthonormal. Therefore, the amplitude matrix can be obtained as

$$\bar{\mathbf{A}}=\bar{\mathbf{\Phi}}^T\mathbf{S} \tag{20}$$

The elements of the amplitude matrix $\bar{\mathbf{A}}$ are then expressed as linear combinations of radial basis functions of the input parameters $\mathbf{k}$ for the complete model. Note that each column of the snapshot matrix $\mathbf{S}$ was obtained for a set $\mathbf{k}^j, j=1,\ldots,M$. Therefore, we write

$$\bar{\mathbf{A}}=\mathbf{BP} \tag{21}$$

where the matrix $\mathbf{B}$ gives the coefficients of the interpolating radial basis functions. Each column of the symmetric matrix $\mathbf{P}$ contains the radial basis functions $p_j(|\mathbf{k}-\mathbf{k}^j|), j=1,\ldots,M$. In this work, the inverse multiquadric radial basis functions (Colaço et al, 2008) were used for the construction of the matrix $\mathbf{P}$, that is,

$$p_j\left(\left|\mathbf{k}-\mathbf{k}^j\right|\right)=\frac{1}{\sqrt{\left|\mathbf{k}-\mathbf{k}^j\right|+c^2}} \tag{22}$$

where c is a smoothing parameter, usually selected as large as possible so that the matrix $\mathbf{P}$ is not ill-conditioned (Ostrowski et al, 2005; Ostrowski et al, 2008; Colaço et al, 2008).

4. RESULTS AND DISCUSSIONS

In this paper, the phase change material was considered as paraffin ($C_{28}H_{58}$) containing copper nanoparticles, initially at the uniform temperature of 313.15 K and with a uniform 1% volume concentration. The geometry for this problem is a square cavity with size 0.3 m, as shown by Fig. 1. The following physical properties are given by Tab. 1.

Table 1. Physical Properties (Lin, S. C., and Al-Kayiem, 2012).

$T_0=313.15$ K,	$T_m=332.78$ K,	$T_{eut}=318.15$ K,	$C_{eut}=0.01\ wt\%$,
$C_p=2378$ J kg^{-1} K^{-1},	$L=160.3$ kJ/kg,	$\rho=922$ kg/m^3,	$k=0.196$ Wm^{-1}K^{-1},
$D_l=6.868\times10^{-12}$ m^{2}s^{-1},	$D_s=6.868\times10^{-19}$ m^{2}s^{-1},	$\kappa=0.45$,	$\mu_l=3.34\times10^{-3}$ kg m^{-1}s^{-1},
$\mu_s=3.34\times10^{4}$ kg m^{-1}s^{-1},	$\beta_T=4\times10^{-5}$ K^{-1},	$\beta_S=0.025$	

Figure 4a presents a comparison of the temperatures computed with the complete model by using 24x24 volumes and 32x32 volumes, at Point 6 (see figure 1, x = 0.075 m and y = 0.3 m), where large temperature variations take place. As the number of finite volumes is increased, the oscillations observed with the coarser grid tends to decrease and the solution becomes smoother. Figure 4a shows that the grid is not fully converged with 24x24 volumes at Point 6, but the agreement between the solutions obtained with these two grids is much better at other positions, such as illustrated by Figure 4b, for Point 4 (x = 0.3 m , y = 0.225 m). Since the objective of this paper is to apply the POD-RBF surrogate solution to the thermal storage system, and the computational times needed to generate the snapshots with the coarser grid were much smaller than those with the finer grid, we used 24x24 finite volumes for the numerical solution of the complete model, with an integration time step of 0.05 seconds. The final time used for the simulations was 24 hours. The convergence criteria of the iterative procedure at each time step was based on the mass source within each control volume, as well as on the discrepancies in the overall energy and solute balances (Colaço and Dulikravich, 2007; Orlande et al, 2017). Each simulation performed with the Fortran code developed in this work for the complete model took around 12 hours of computational time, in an Intel®Core™ i7-2600CPU@3.4GHz with 16GB of RAM, compiled with 64-bit Linux gfortran. The computational time for the solution with the POD-RBF surrogate model was around 1 minute, which resulted in a speedup of 720.

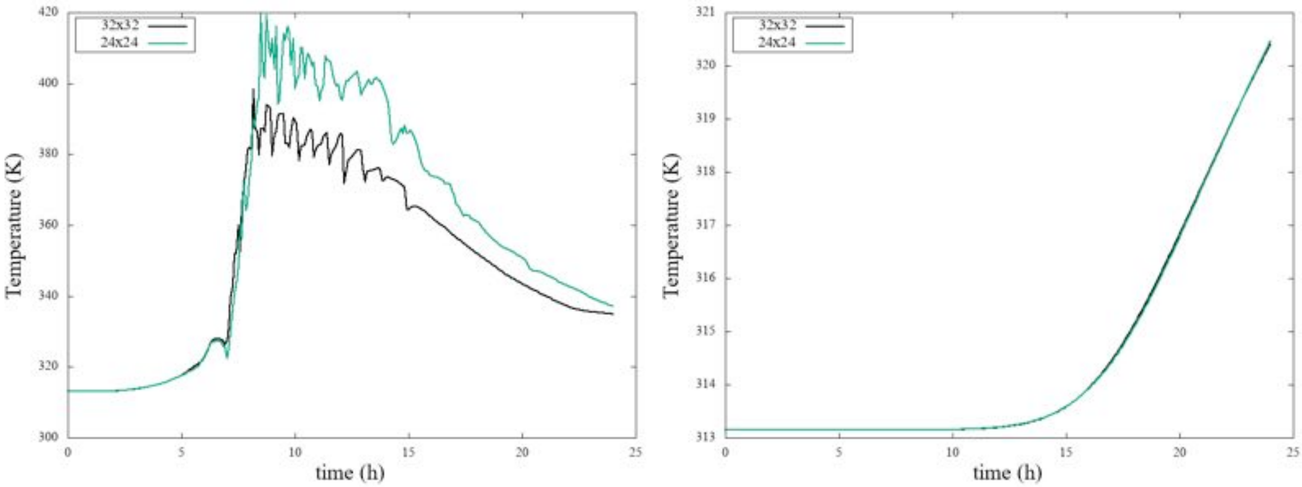

(a) (b)

Figure 4. Comparison between complete model solutions obtained with two different finite volume grids at: (a) Point 6 (x = 0.075 m , y = 0.3 m), (b) Point 4 (x = 0.3 m , y = 0.225 m).

Each snapshot was a vector of 290 transient temperatures, taken every 5 minutes in the 24 hour period of simulation, at the 6 positions represented by the gray dots in Figure 1. A total of $M = 100$ snapshots were generated for a random input heat flux, which was obtained from a Gaussian distribution centered on the values shown by figure 2 and with a standard deviation of 10% of these mean values. To solve the required linear systems to obtain the RBF coefficients, we used the routine DGESDD from the LAPACK library for FORTRAN (Anderson et al, 2006). The truncated POD basis matrix, $\overline{\Phi}$, consisted of 50 vectors (modes), due to the decay of the eigenvalues of the complete POD basis matrix.

Figures 5a to 5f present a comparison of the solutions obtained with the complete model and with the surrogate POD-RBF model, at the six positions where the snapshots were considered, respectively. The heat flux used to obtain the results presented in Figs. 5a-f was that given by Fig. 2. Figures 5a-f shows an excellent agreement between the POD-RBF solutions and the complete model solutions at the graph scale, despite the complex physical phenomena accounted for in the complete model. However, we notice small discrepancies between the complete and surrogate solutions for large times at point 5 (Fig. 5e) and at point 6 (Fig. 5f). Points 5 and 6 are located at the top boundary. Together with point 1 at the bottom boundary, points 5 and 6 exhibit the largest temperature variations during the time interval of 24 h in the snapshots used to generate the POD-RBF solution. In particular, the POD-RBF solution does not follow the numerical oscillations at point 6, because the truncated basis used in this work filters out the high frequencies (Ostrowski, 2006; Rogers et al, 2012; Rogers, 2008; Ostrowski et al, 2005; Ostrowski et al, 2008).

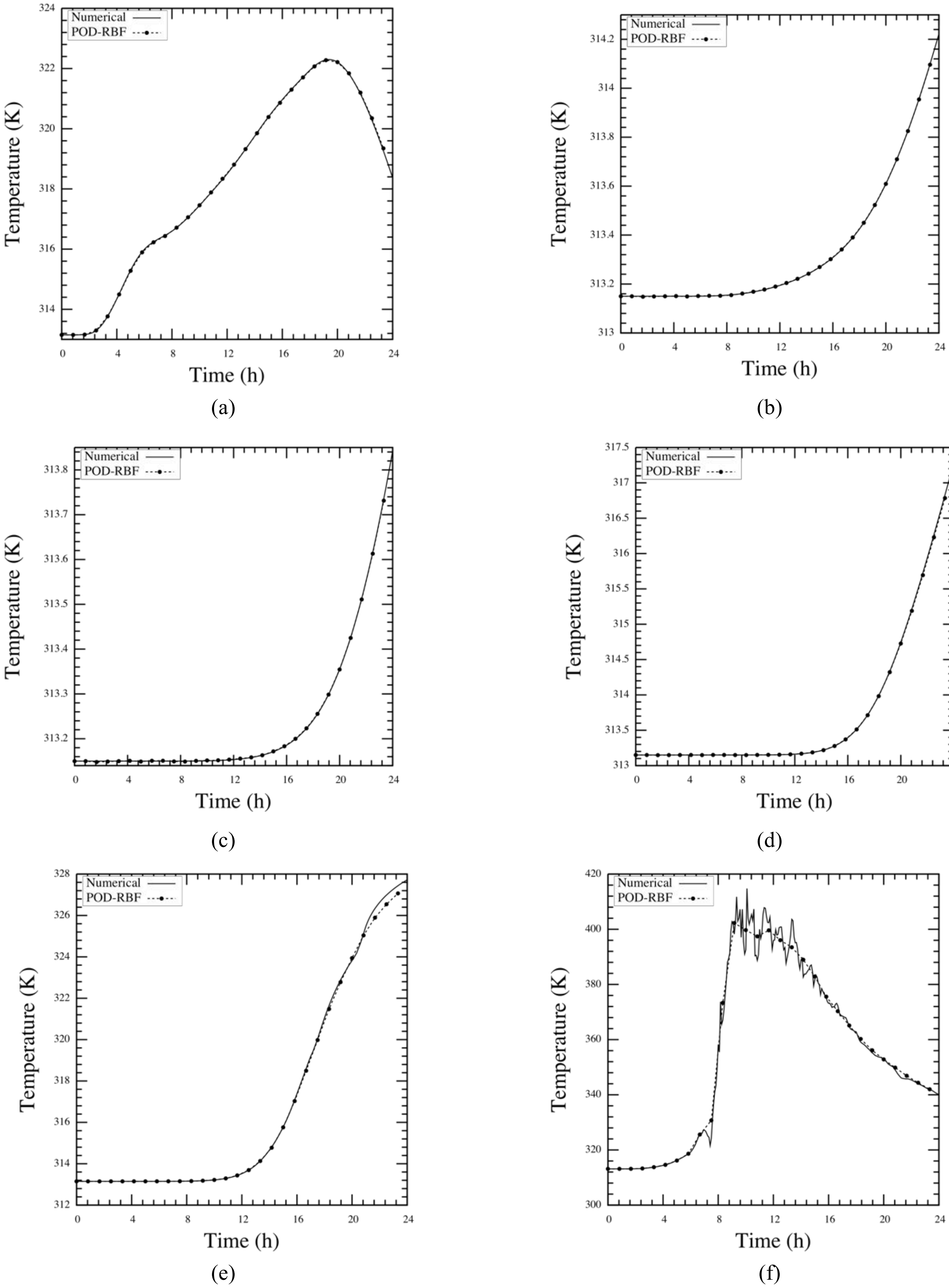

Figure 5. Comparison between complete model and surrogate model solutions at: (a) Point 1 (x = 0.075 m , y = 0 m), (b) Point 2 (x = 0.225 m , y = 0 m), (c) Point 3 (x = 0.3m , y = 0.075m), (d) Point 4 (x = 0.3 m , y = 0.225 m), (e) Point 5 (x = 0.225 m , y = 0.3 m) and (f) Point 6 (x = 0.075 m , y = 0.3 m).

Finally, Figs. 6a and 6b were prepared to illustrate the accuracy of the POD-RBF surrogate solution for a heat flux randomly selected from the Gaussian distribution used to generate the snapshot matrix. Figures 6a and 6b present a comparison of the complete model and surrogate model solutions, at points 5 and 6, respectively, for the heat flux presented by Fig. 7. An analysis of Figs. 6a and 6b reveals the capabilities of the RBF interpolation of the POD basis, which resulted in accurate solutions for a noisy input heat flux.

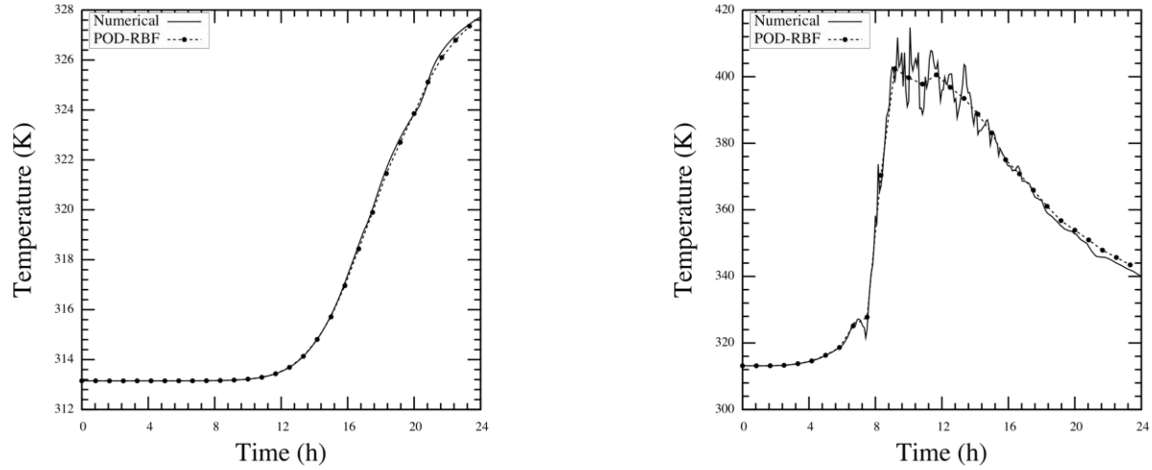

(a) (b)

Figure 6. Complete and surrogate solutions obtained with the heat flux presented by figure 7 at:
(a) Point 5 (x = 0.225 m , y = 0.3 m) and (b) Point 6 (x = 0.075 m , y = 0.3 m).

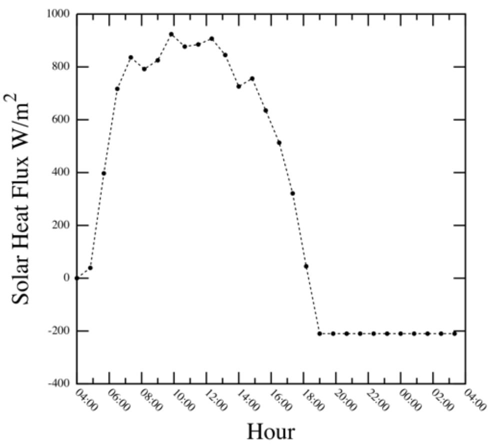

Figure 7. Noisy input heat flux used for the comparison presented by figure 6.

5. CONCLUSIONS

5. CONCLUSIONS

In this work we presented a surrogate solution for a two-dimensional phase change problem, based on the Proper Orthogonal Decomposition (POD) and a Radial Basis Function (RBF) interpolation of the POD matrix. The snapshots were generated from a random input heat flux, with a Gaussian distribution centered on the typical solar irradiation for the city of Rio de Janeiro in February. The complete model took into account the advection and diffusion of nanoparticles in the phase change material, as well as the natural convection in the liquid phase. Despite the complex physical phenomena in the complete model, the POD-RBF model was capable of accurately representing the temperatures at six different locations at the boundaries, which were used to generate the snapshots, with a computational speedup of 360.

6. ACKNOWLEDGEMENTS

The authors would like to thank the Brazilian agencies for the fostering of science, Conselho Nacional de Desenvolvimento Científico e Tecnológico (CNPq), Coordenação de Aperfeiçoamento de Pessoal de Nível Superior

(CAPES, Finance Code 001) and Fundação Carlos Chagas Filho de Amparo à Pesquisa do Estado do Rio de Janeiro (FAPERJ), for the financial support for this work.

7. REFERENCES

Anderson, E., Bai, Z., Bischof, C., Blackford, S., Demmel, J., Dongarra, J., Du Croz, J., Greenbaum, A., Hammarling, S., McKenney, A., and Sorensen, D., 1999, LAPACK Users' Guide, Society for Industrial and Applied Mathematics, Philadelphia, PA.

Colaço, M. J., Orlande, H. R. B., and Dulikravich, G. S., 2006, "Inverse and Optimization Problems in Heat Transfer". *J. Brazilian Soc. Mech. Sci. Eng*., Vol. 28, No. 1, pp. 1–24.

Colaço, M. J., and Dulikravich, G. S., 2007, "Solidification of Double-Diffusive Flows Using Thermo-Magneto-Hydrodynamics and Optimization". Mater. Manuf. Process., Vol. 22, No. 5, pp. 594–606.

Colaço, M. J., Dulikravich, G. S., and Sahoo, D., 2008, "A Response Surface Method-Based Hybrid Optimizer". *Inverse Probl. Sci. Eng.*, Vol. 16, No. 6, pp. 717–741.

Dhaidan, N. S., Khodadadi, J. M., Al-Hattab, T. A., and Al-Mashat, S. M., 2013, "Experimental and Numerical Investigation of Melting of Phase Change Material/Nanoparticle Suspensions in a Square Container Subjected to a Constant Heat Flux". *Int. J. Heat Mass Transf.*, Vol. 66, pp. 672–683.

Fernandes, D., Pitié, F., Cáceres, G., and Baeyens, J., 2012, "Thermal Energy Storage: 'How Previous Findings Determine Current Research Priorities". *Energy, Vol*. 39, No. 1, pp. 246–257.

Jaccoud, B.R., Orlande, H.R.B., Colaço, M.J., Fudym, O. and Caldeira, A.B., 2018. "State estimation for the thermal storage in phase change materials containing nanoparticles". *High Temperatures-High Pressures*, Vol. 47, pp. 117-137.

Lin, S. C., and Al-Kayiem, H. H., 2012, "Thermophysical Properties of Nanoparticles-Phase Change Material Compositions for Thermal Energy Storage". *Appl. Mech. Mater*., Vol. 232, pp. 127–131.

Miller, F. M., and Colaço, M. J., 2016, "Concentrating Linear Fresnel Reflector Working with Supercritical CO2 Power Cycles", In *11th Conference on Sustainable Development of Ener*gy, Lisbon, Portugal.

Orlande, H. R. B., Fudym, O., Maillet, D., and Cotta, R. M., 2011, *Thermal Measurements and Inverse Techniques*, CRC Press, Boca Raton, FL.

Orlande, H. R., Özişik, M. N., Colaço, M. J., and Cotta, R. M., 2017, *Finite Difference Methods in Heat Transfer*, CRC Press.

Ostrowski, Z., 2006, *Application of Proper Orthogonal Decomposition to the Solution of the Inverse Problem*, Ph.D. Thesis, Silesian University of Technology, Poland.

Ostrowski, Z., Białecki, R. A., and Kassab, A. J., 2005, "Estimation of Constant Thermal Conductivity by Use of Proper Orthogonal Decomposition," *Comput. Mech*., **37**(1), pp. 52–59.

Ostrowski, Z., Białecki, R. A., and Kassab, A. J., 2008, "Solving Inverse Heat Conduction Problems Using Trained POD-RBF Network Inverse Method," *Inverse Probl. Sci. Eng*., **16**(1), pp. 39–54.

Özışık, M. N., and Orlande, H. R. B., 2000, *Inverse Heat Transfer: Fundamentals and Applications*, Taylor & Francis.

Rappaz, M., 1989, "Modelling of Microstructure Formation in Solidification Processes". *Int. Mater. Rev*., Vol. 34, No. 1, pp. 93–124.

Rogers, C. A., Kassab, A. J., Divo, E. A., Ostrowski, Z., and Bialecki, R. A., 2012, "An Inverse POD-RBF Network Approach to Parameter Estimation in Mechanics". *Inverse Probl. Sci. Eng*., Vol. 20, No. 5, pp. 749–767.

Rogers, C. A., 2008, *Parameter Estimation in Heat Transfer and Elasticity Using Trained POD-RBF Network Inverse Methods*, Ph.D. thesis, University of Central Florida, USA.

Voller, V. R. R., Brent, A. D. D., and Prakash, C., 1989, "The Modeling of Heat Mass and Solute Transport in Solidification Systems". *Int. J. Heat Mass Transf.,* Vol. 32, No. 9, pp. 1719–1731.

Yousef, M. F. E., Khodadadi, J. M. M., El Hasadi, Y. M. F., and Khodadadi, J. M. M., 2013, "One-Dimensional Stefan Problem Formulation for Solidification of Nanostructure-Enhanced Phase Change Materials (NePCM)". *Int. J. Heat Mass Transf.*, Vol. 67, pp. 202–213.

8. RESPONSIBILITY NOTICE

The authors are the only responsible for the printed material included in this paper.